Article

Journal of
Nanoscience and Nanotechnology
Vol. 19, 613–621, 2019
www.aspbs.com/jnn

Intracellular Delivery of Nanoparticles Mediated by Lactoferricin Cell-Penetrating Peptides in an Endocytic Pathway

Han-Jung Lee[1,*], Yue-Wern Huang[2], and Robert S. Aronstam[3]

[1] *Department of Natural Resources and Environmental Studies, National Dong Hwa University, Hualien 97401, Taiwan*
[2] *Department of Biological Sciences, Missouri University of Science and Technology, Rolla, MO 65409-1120, USA*
[3] *College of Science and Technology, Bloomsburg University of Pennsylvania, Bloomsburg, PA 17815-1301, USA*

Cell-penetrating peptides (CPPs) containing a preponderance of basic amino acids are able to deliver biologically active macromolecules and nanomaterials into live cells. Quantum dots (QDs) are nanoparticles with unique fluorescence properties that have found wide application in biomedical imaging. In this study, we demonstrate transduction of an L6 CPP (RRWQWR) derived from bovine lactoferricin (LFcin) into human lung cancer cells. L6 noncovalently interacts with QDs to form stable complexes. L6/QD complexes enter cells most efficiently when prepared at a nitrogen/phosphate ratio of 60. Mechanistic studies indicate that L6/QD complexes enter cells by endocytosis. Treatment with 1,2-benzisothiazol-3(2*H*)-one (BIT), an industrial preservative that enhances uptake of certain CPPs, does not affect L6 CPP-mediated protein transduction efficiency. L6 and L6/QD complexes are not cytotoxic. These results indicate that L6 LFcin might be an efficient and safe nanoshuttle for nanoparticles or nanomedicines in biomedical applications.

Keywords: Cell-Penetrating Peptides, Lactoferricin, Nanoparticles, Protein Transduction, Quantum Dots.

1. INTRODUCTION

Protein transduction using cell-penetrating peptides (CPPs), also known as protein transduction domains (PTDs), is a useful method to deliver macromolecules into cells.[1] CPPs comprise a diverse class of short peptides (less than thirty amino acids) that readily enter cells. The original discovery of CPPs derived from the ability of the HIV-1 transactivator of transcription (Tat) protein to enter cells.[2,3] An eleven-amino acid sequence rich in basic amino acids (YGRKKRRQRRR) in the 86-amino acid Tat is, and is essential for Tat translocation through the plasma membrane.[4] A variety of amphipathic, hydrophobic, and cationic peptides with cell-penetrating properties (i.e., CPPs) have now been identified. These CPPs traverse cell membranes and can mediate the cotransport of a wide range of biological molecules and chemical compounds into cells.[5] Cargos that can be delivered by CPPs include nucleic acids, proteins, and nanomaterials. About 1,700 CPP sequences have been deposited in the database CPPsite 2.0.[6] The CPPpred, CellPPD, and C2Pred bioinformatic platforms provide technical models that predict CPP effectiveness.[7–9] The number of publications and clinical trials with CPPs is increasing.[10] Clinical data are available from twenty-five completed Phase I and II clinical trials that evaluated the efficacy and safety of CPP-mediated delivery of macromolecules *in vivo*.[1] An ongoing Phase III clinical trial utilizes Tat PTD-mediated delivery of botulinum toxin type A to treat lateral canthal lines.[1,11]

Despite recent advances in the CPP field, uncertainty regarding the uptake mechanisms and intracellular trafficking of CPP-mediated protein transduction remains. Studies have suggested multiple pathways for cellular entry of CPPs and CPP/cargo complexes; both endocytosis and direct membrane translocation have been implicated.[12,13] Endocytosis encompasses active transport pathways, including phagocytosis and pinocytosis.[14] Pinocytosis includes four subcategories: macropinocytosis (a lipid raft process), and clathrin-dependent, caveolin-dependent, and

*Author to whom correspondence should be addressed.

clathrin/caveolin-independent pathways.[14] The first step of protein transduction into cells involves the binding of CPPs to cell membranes.[10] Binding partners of positively charged CPPs include negatively charged proteoglycans present on most cell surfaces, such as heparin sulfate.[15] Various physical and pharmacological endocytic inhibitors have been used to identify potential pathways for CPP-mediated protein transduction. For instance, 5-(*N*-ethyl-*N*-isopropyl)-amiloride (EIPA) specifically inhibits macropinocytosis by restraining Na^+/H^+ exchange.[16] The endocytic inhibitor cytochalasin D (CytD), an F-actin polymerization disrupter, perturbs endocytic processes that involve clathrin-, caveolae-dependent endocytosis and macropinocytosis.[17] Filipin III (FIL) inhibits lipid raft-dependent caveolae endocytosis,[18] while nocodazole (NCO) inhibits clathrin-dependent endocytosis.[13] Low temperature (4 °C) treatment arrests all energy-dependent movement across the cell membrane.[16] Recently, 1,2-benzisothiazol-3(2*H*)-one (BIT), a commonly used biocide, was identified as a chemical enhancer of the cellular uptake of Tat PTD and PTD-green fluorescent protein (GFP) fusion protein by increasing membrane permeability without engendering membrane perforation.[19]

Quantum dots (QDs) are colloidal, light-emitting nanocrystals that are finding increasing use in cellular imaging.[20] QDs possess unique chemical and physical properties, including high photoluminescent quantum efficiency, photostability, tunability, narrow emission spectrum, and prolonged fluorescence lifetime.[21] Although QDs are useful in biomedical imaging studies, they do not readily enter cells, and aggregation often occurs before and after internalization.[22] The size and inorganic nature of QDs make delivery into the cytosol difficult.[23] However, CPPs have been used to facilitate intracellular delivery of QDs that have been surface-functionalized with carboxyl groups to reduce nonspecific absorption between CPPs and QDs and to increase QD water solubility.[24–26]

While six to twelve arginine residues are optimal for efficient protein transduction activity of CPPs,[27,28] it has been reported that as few as three arginines may be sufficient for protein transduction.[29] We recently identified several CPP candidates derived from bovine lactoferricins (LFcins).[30] Among these are L6 (RRWQWR) LFcin, a short CPP that is capable of delivering DNA into cells. However, little is known about the mechanism of action of L6 LFcin. Accordingly, the aims of this study were to (1) demonstrate cellular internalization of QDs mediated by L6 CPP, (2) elucidate the cellular uptake mechanism of L6/QD complexes, and (3) determine the effect of BIT on cellular uptake of L6/QD complexes.

2. EXPERIMENTAL DETAILS

2.1. Preparation of Peptides and QDs

L6 (RRWQWR) and *N*-labeled L6-fluorescein isothiocyanate (FITC) peptides were purchased from Genomics (Taipei, Taiwan), while nonCPP bradykinin-FITC (RPPGFSPFR) peptide[31] was purchased from GMbiolab Co. (Taichung, Taiwan). Trilite fluorescent nanocrystal QDs (FN-525-C-25MG) were purchased from Cytodiagnostics (Burlington, Ontario, Canada). Carboxyl-functionalized QDs with a diameter of 5.5–6.5 nm are water soluble and possess a maximal emission peak wavelength of 525 ± 5 nm.

2.2. Gel Retardation Assay

To characterize noncovalent interactions between CPPs and QDs, various amounts of L6 (from 0 to 15 μM) were incubated with 0.2 μM of QDs at 37 °C for 1 h. Complexes formed at molecular nitrogen (NH_3^+)/phosphate (PO_4^-) (N/P) ratios[32] of 0 (QDs alone), 15, 30, 45, 60, and 75 were analyzed by electrophoresis on a 1% SeaKem Gold agarose gel (Lonza Group, Basel, Switzerland) in 0.5× TBE buffer (44.5 mM of Tris-borate and 1 mM of EDTA, pH 8.3) at 50 V for 30 min.[30] Gel images were captured using a ChemiDoc XRS+gel imaging system (Bio-Rad, Hercules, CA, USA) with an excitation wavelength of 302 nm and an emission wavelength range of 548–630 nm. Data were analyzed using Quantity One 1-D analysis software 4.6.9 (Bio-Rad). The shift of the QD band migrating in the gel was quantified as a reciprocal mobility ratio normalized to scale in which the minimal N/P ratio of 0 was 0%, and the maximal N/P ratio of 75 was 100%.

2.3. Cell Culture

Human bronchoalveolar carcinoma A549 cells (American Type Culture Collection, Manassas, VA, USA; CCL-185) were cultured in Gibco RPMI 1640 medium (Thermo Fisher, Waltham, MA, USA) supplemented with 10% (v/v) Gibco fetal bovine serum (Thermo Fisher), 1× antibiotic-antimycotic solution (Caisson Labs, Smithfield, UT, USA), and 0.5 μl/ml of Cellmaxin (GenDEPOT, Katy, TX, USA). Cells were washed with phosphate buffered saline (PBS), and switched to serum-free RPMI 1640 medium for protein transduction experiments.[33] Cells were maintained at 37 °C and 5% CO_2 in a humidified incubator.

2.4. Noncovalent Protein Transduction

For cellular internalization analysis, A549 cells were seeded at a density of about 1×10^5 per 35-mm petri dish and then treated with either PBS (control), 80 μM of bradykinin-FITC, or L6-FITC at 37 °C for 1 h. Cells were stained with the nucleus-specific fluorescent tracker Hoechst 33342, according to the manufacturer's instructions (Thermo Fisher). Non-transduced QDs or L6/QD complexes were removed from cell surface by washing with PBS. To analyze noncovalent protein transduction between CPPs and QDs, 6 μM of L6 peptides were premixed with 0.1 μM of QDs at a molecular N/P ratio of 60 at 37 °C for 1 h. Following complex formation, the mixtures were incubated with A549 cells at 37 °C for

an additional 1 h.[33] To study the influence of the chemical enhancer BIT in protein transduction efficiency, cells were treated with QDs alone or L6/QD complexes prepared at an N/P ratio of 60 in the absence or presence of 0.65 mM BIT (Sigma-Aldrich, St. Louis, MO, USA) at 37 °C for 1 h.

2.5. Subcellular Colocalization

To determine subcellular colocalization, cells were treated with QDs alone or L6/QD complexes prepared at an N/P ratio of 60 at 37 °C for 1 h, followed by organelle-marker staining according to the manufacturers' instructions. Specifically, the cells were treated with 16.2 μM Hoechst 33342 at 37 °C for 30 min, 50 nM Texas Red-X phalloidin at 37 °C for 30 min, 50 nM LysoTracker Red DND-99 at 37 °C for 30 min, 50 nM MitoTracker Deep Red FM at 37 °C for 30 min, 1 μM ER-Tracker Red (Thermo Fisher) at 37 °C for 30 min, 10^3 diluted rabbit anti-human early endosome antigen 1 protein (EEA1) monoclonal antibody at 37 °C for 1 h and goat anti-rabbit IgG F(ab′)$_2$ Alexa Fluor 647-conjugated antibody (Cell Signaling Technology, Danvers, MA, USA) at 37 °C for 1 h, and 5 μg/ml FM 4-64 (Thermo Fisher) at 4 °C for 1 min to visualize nuclei, cytoskeleton, lysosomes, mitochondria, endoplasmic reticula, EEA1, and membranes, respectively.[34, 35]

2.6. Mechanistic Studies of Cellular Uptake

To determine potential cellular uptake pathways, low temperature (4 °C) and a series of pharmacological modulators (EIPA, CytD, FIL, and NCO) were used. For low temperature treatment, cells were pretreated at 4 °C for 30 min, and then treated with QDs alone or L6/QD complexes prepared at an N/P ratio of 60 at 4 °C for an additional 30 min.[35] For pharmacological treatments, cells were treated with QDs alone or L6/QD complexes in the absence or presence of 100 μM EIPA, 10 μM CytD, 5 μg/ml FIL, or 10 μM NCO (Sigma-Aldrich) at 37 °C for 1 h.[35]

2.7. Fluorescent Microscopy

Fluorescent and bright-field images were recorded using an AE31 inverted Epi-fluorescence microscope (Motic, Causeway Bay, Hong Kong) with an IS1000 eyepiece (Tucsen, Fujian, China). Excitation filters were set at 480/30, 350/50, and 560/40 nm for GFP, blue (BFP), and red fluorescent protein (RFP) channels, respectively, while emission filters were set at 535/40, 460/50, and 630/60 nm for GFP, BFP, and RFP channels, respectively. Bright-field images were used to observe cell morphology. The intensity of fluorescent images was quantified using ImageJ software.[36] Overlapped fluorescence-images were stacked using Startrails software (http://www.startrails.de/).

2.8. Cytotoxicity Assay

To assess the cytotoxicity of L6, QDs, and L6/QD complexes, A549 cells were treated at 37 °C for 24 h with 6 μM of L6 alone, 0.1 μM of QDs alone, or L6/QD complexes prepared at an N/P ratio of 60. Cells were treated with serum-free medium and 100% dimethyl sulfoxide (DMSO) for 24 h as negative and positive controls, respectively. The colorimetric 3-(4,5-dimethylthiazol-2-yl)-2,5-diphenyltetrazolium bromide (MTT) dye reduction assay was performed as previously described.[30]

2.9. Statistical Analysis

Data are expressed as mean ± standard deviation (SD) from at least three independent experiments carried out in triplicates for each treatment group. Statistical comparisons were performed by ANOVA and the Student's *t*-test, using levels of statistical significance of $P < 0.05$ (∗) or 0.01 (∗∗), as indicated.

3. RESULTS

3.1. Cellular Internalization of L6 LFcin

To assess cellular internalization of L6 LFcin, human A549 cells were treated with L6-FITC, followed by staining with Hoechst 33342, and then analyzed using fluorescent microscopy. Green fluorescence was detected in the cells treated with L6-FITC (Fig. 1). In contrast, almost no GFP channel fluorescence was seen either in internal control cells or cells treated with negative control bradykinin-FITC. These results are consistent with our previous observations.[30] Accordingly, L6 was tested as a shuttle CPP to deliver QDs into cells in subsequent experiments.

3.2. Interactions Between L6 CPPs and QDs *In Vitro*

Agarose-based gel retardation assays were conducted to determine whether L6 CPPs form stable, noncovalent complexes with QDs. Various amounts of L6 were incubated with QDs at N/P ratios from 0 to 75. QDs exhibited a reduced mobility when incubated with L6 CPPs, and the mobility decreased as the concentration of L6 was increased (Fig. 2(a)). Relative shift analysis revealed that ratio-dependent interactions of L6/QD complexes were maximal at N/P ratios above 45 (Fig. 2(b)). Accordingly, an N/P ratio of 60 was used in subsequent experiments.

3.3. CPP-Mediated Intracellular Delivery of QDs

To determine whether L6 CPPs can deliver QDs into cells, L6/QD complexes prepared at an N/P ratio of 60 were incubated with A549 cells, followed by staining with Hoechst 33342, and analysis using fluorescent microscopy. Green fluorescence was observed in the cells treated with L6/QD complexes, but not in the cells treated with QDs alone (Fig. 3(a)). These results indicate that L6 CPPs are able to efficiently deliver QDs into cells.

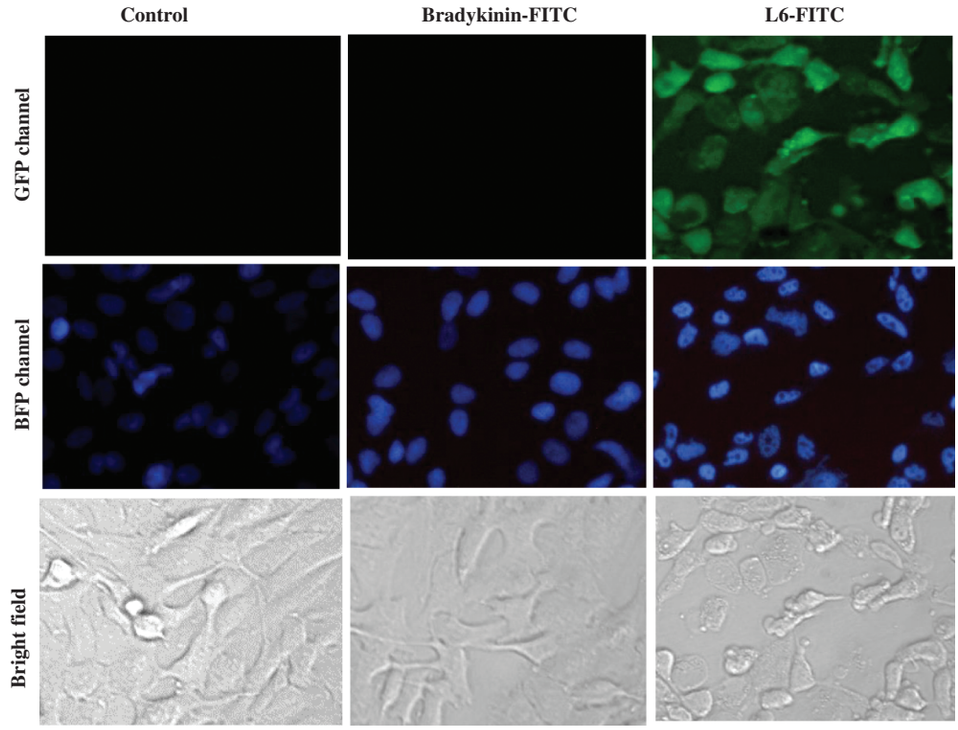

Figure 1. Cellular internalization of CPP-FITC. A549 cells were treated with L6-FITC for 1 h, and then stained with Hoechst 33342. Cells were treated with serum-free medium and bradykinin-FITC as internal and negative controls, respectively. GFP, BFP channels and bright fields revealed the distribution of L6-FITC, nuclei, and cell morphologies, respectively. All images are obtained using a Motic AE31 fluorescent microscope with a magnification of 200×.

To investigate whether BIT influences CPP-mediated QD delivery, cells were treated with L6/QD complexes prepared at an N/P ratio of 60 in the presence of BIT. In a quantitative analysis of fluorescent intensity, green fluorescence was higher in cells exposed to L6/QD complexes than in control cells in the absence or presence of BIT (Fig. 3(b)). However, protein transduction efficiency mediated by L6/QD was not affected by BIT; additive or synergistic effects were not observed.

3.4. Subcellular Distribution of L6/QD Complexes

To investigate the subcellular distribution of L6-delivered QDs, cells were treated with QDs alone or with L6/QD complexes, and stained with organelle-specific fluorescent

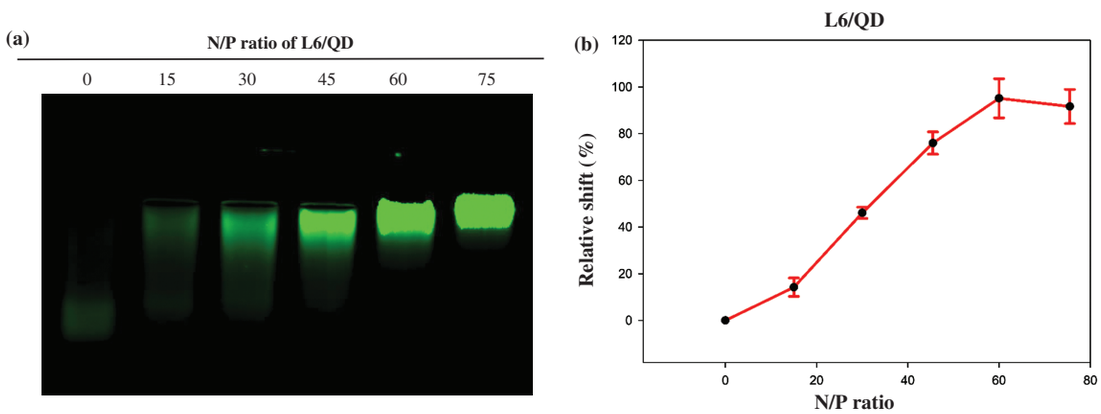

Figure 2. Noncovalent interactions between CPPs and QDs. (a) Gel retardation assay. Various amounts of L6 were incubated with QDs at molecular N/P ratios of 0 (QDs alone), 15, 30, 45, 60, and 75. These complexes were analyzed by electrophoresis on a 1% agarose gel, and images were captured using a ChemiDoc XRS + gel imaging system (Bio-Rad). (b) The relative mobility of L6/QD complexes prepared at different N/P ratios. The mobility of L6/QD complexes is indicated. Data are analyzed using the Quantity One 1-D analysis software (Bio-Rad) and presented as mean ± SD from four independent experiments for each treatment group.

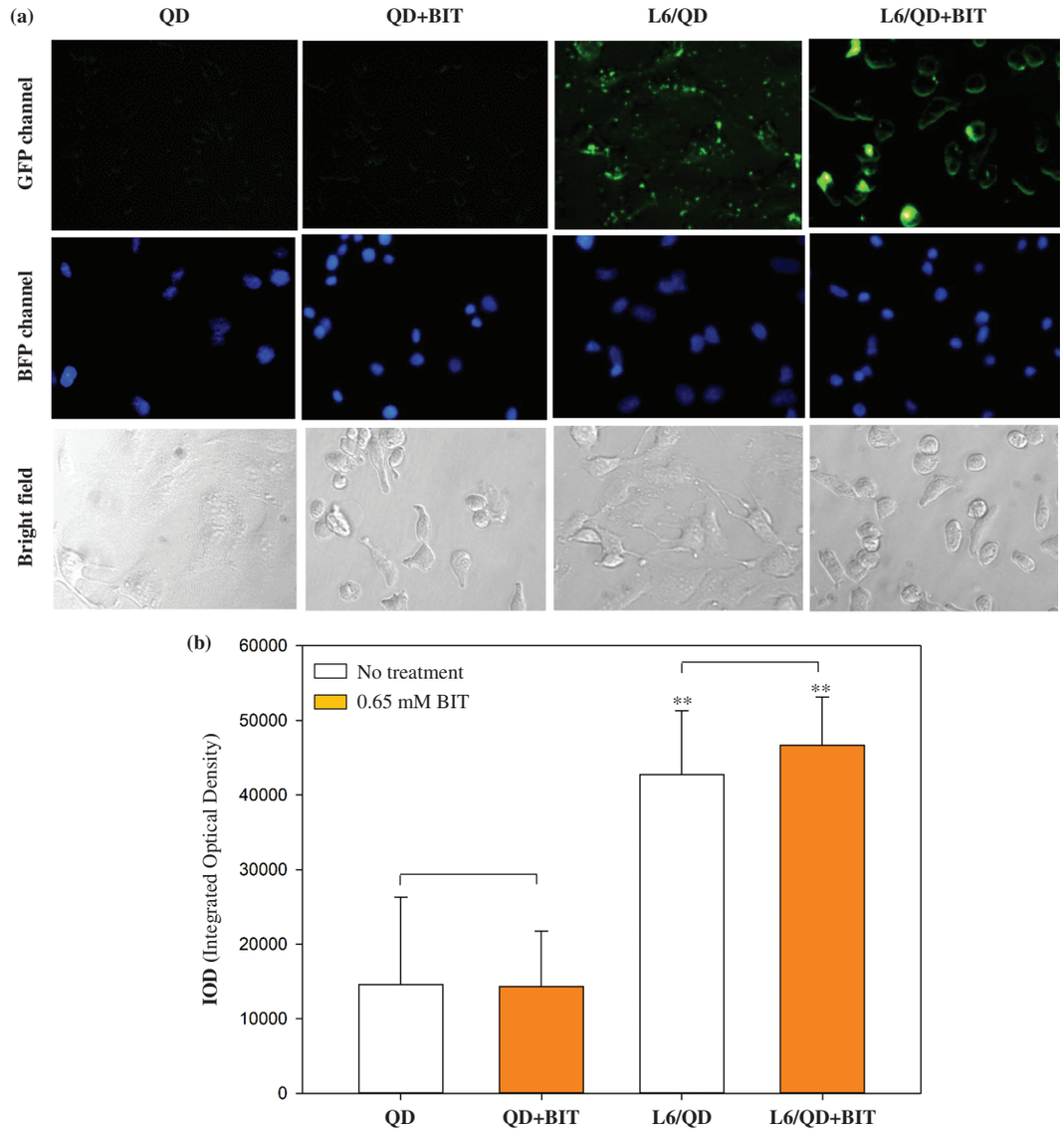

Figure 3. CPP-mediated cellular internalization of QDs. (a) Images of L6-mediated delivery of QDs into cells in the absence or presence of BIT. QDs alone and L6/QD complexes prepared at an N/P ratio of 60 were incubated with cells for 1 h in the absence or presence of 0.65 mM BIT, followed by staining with Hoechst 33342. BFP and GFP channels revealed the distribution of nuclei and QDs, respectively. Cell morphologies were observed in bright-field images using a Motic AE31 fluorescent microscope with a magnification of 200×. (b) Effect of BIT on CPP-mediated cellular uptake of QDs. Fluorescent intensity recorded in panel A was quantified using ImageJ. Data are presented as mean ± SD from four independent experiments for each treatment group. Experimental L6/QD groups were compared with QD groups, and each group without BIT treatment was compared with the group with BIT treatment. Significant differences at $P < 0.01$ (**) are indicated.

markers, namely Hoechst 33342, Texas Red-X phalloidin, LysoTracker Red DND-99, MitoTracker Deep Red FM, ER-Tracker Red, EEA1 antibody, and FM 4-64 for the visualization of nuclei, cytoskeleton, lysosomes, mitochondria, endoplasmic reticula, EEA1, and membranes, respectively. In most cells, merged images demonstrated that QDs alone were not taken up to any appreciable extent, and were not associated with any particular organelle marker (Fig. 4). However, some yellow spots were observed in the merged images of L6/QD groups in lysosomes, early endosomes, and membranes, indicating association of QDs with these localizations following L6-mediated transduction delivery. This distribution is consistent with the involvement of endocytosis in the cellular internalization of L6/QD complexes.

3.5. Molecular Mechanism of Cellular Uptake of L6/QD Complexes

To reveal the mechanism of L6-mediated cellular delivery of QDs, a series of inhibition studies were conducted.

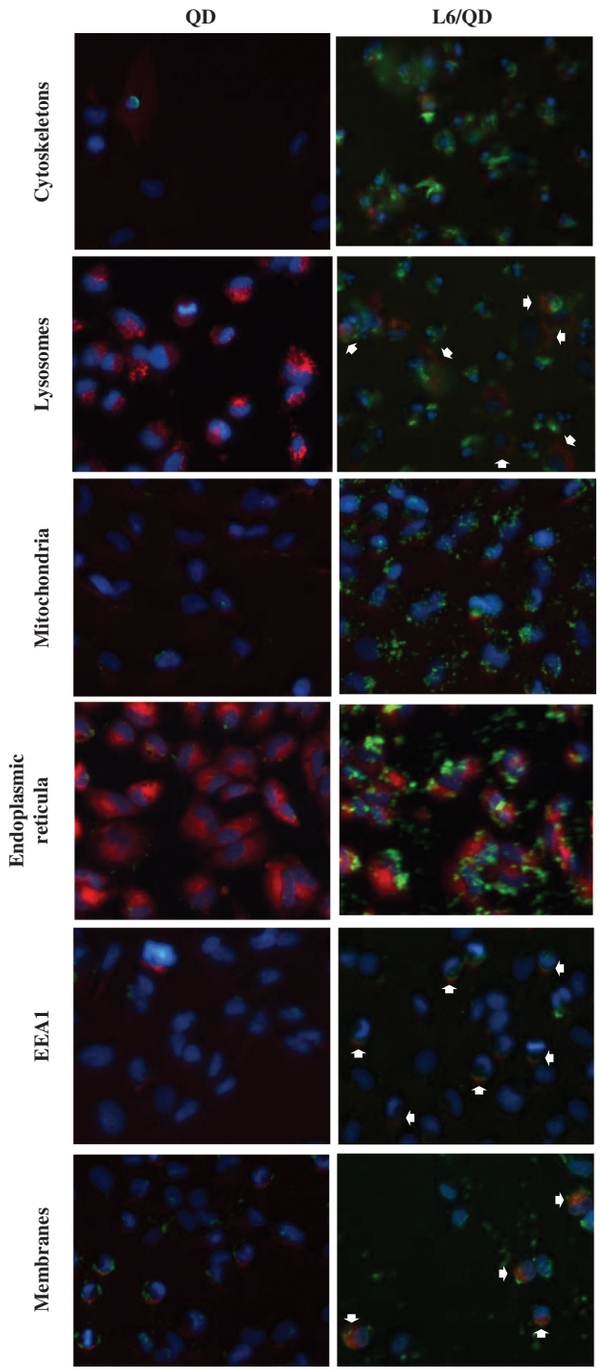

Figure 4. Intracellular colocalization of CPP/QD complexes with organelles. A549 cells were treated with QDs alone or L6/QD complexes for 1 h and then stained with Hoechst 33342 for nuclei, Texas Red-X phalloidin for cytoskeleton, LysoTracker Red DND-99 for lysosomes, MitoTracker Deep Red FM for mitochondria, ER-Tracker Red for endoplasmic reticula, rabbit anti-human EEA1 monoclonal antibody and goat anti-rabbit Alexa Fluor 647-conjugated antibody for EEA1, or FM 4-64 for membranes. An overlap of QDs and organelle trackers is yellow in merged GFP and RFP images. An overlap of QDs and nuclei is cyan in merged GFP and BFP images. All fluorescent images are shown at a magnification of 200×.

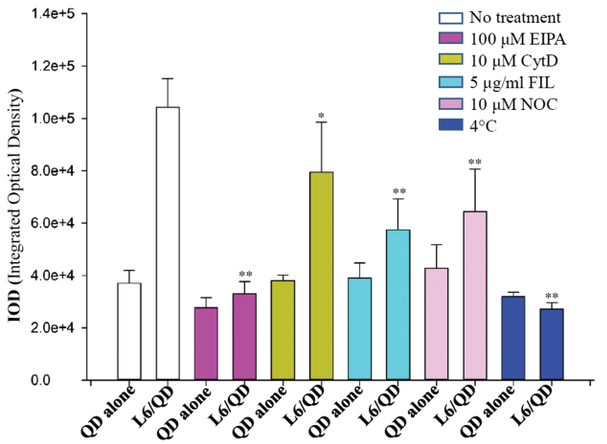

Figure 5. Effect of endocytic modulators on cellular internalization of CPP/QD complexes. Cells were treated with QDs alone or L6/QD complexes in the absence or presence of the endocytic inhibitors EIPA, CytD, FIL, or NCO, or incubated at 4 °C. After treatment for 1 h, the cells were analyzed by fluorescent microscopy, and fluorescent intensity was quantified using ImageJ. Significant differences of $P < 0.05$ (∗) and $P < 0.01$ (∗∗) are indicated. Data are presented as mean ± SD from five independent experiments for each treatment group.

Cells were treated with QDs alone or L6/QD complexes in the absence or presence of pharmacological inhibitors or at low temperature, followed by fluorescent microscopic analysis. Cellular internalization of L6/QD complexes was inhibited by treatments with EIPA, CytD, FIL, or NCO, and by incubation at 4 °C (Fig. 5). These results indicate

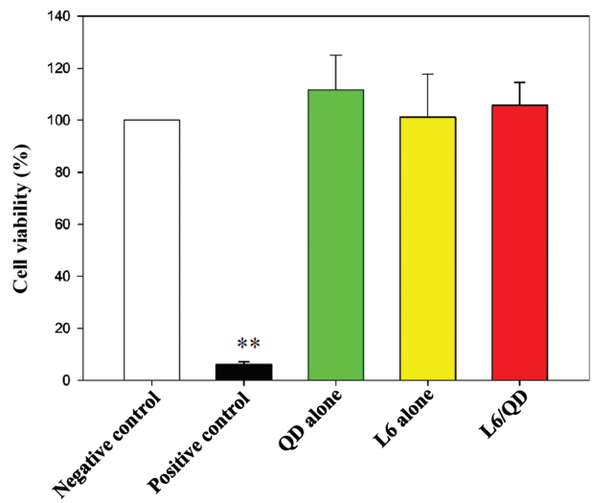

Figure 6. Cytotoxicity of CPPs, QDs, and CPP/QD complexes. Cells were treated with QDs, L6, or L6/QD complexes at 37 °C for 24 h. Cells treated with serum-free medium and 100% DMSO at 37 °C for 24 h served as negative and positive controls, respectively. The MTT assay was used to evaluate cell viability. Significant differences from the negative control at $P < 0.01$ (∗∗) are indicated. Data are presented as mean ± SD from four independent experiments for each treatment group.

that energy-dependent endocytosis is the main route for intracellular delivery of L6/QD complexes.

3.6. Cytotoxicity of L6-Mediated QD Delivery

The MTT assay was used to determine the effect of L6-mediated QD delivery on cell viability. Cells were treated with QDs alone, L6 alone, or L6/QD complexes for 24 h, and then analyzed using the MTT assay. No cytotoxicity was detected in the cells treated with QDs, L6, or L6/QD complexes (Fig. 6).

4. DISCUSSION

In this study, we demonstrate that bovine LFcin L6 can efficiently deliver noncovalently complexed QDs into cells by an endocytic mechanism. L6/QD complexes colocalize with lysosomes, early endosomes, and membranes in cells after protein transduction. BIT, a chemical enhancer of the cellular uptake of Tat PTD, failed to affect L6-mediated intracellular delivery of QDs into cells. Cell viability assay confirmed that neither L6 CPPs nor L6/QD complexes are cytotoxic. In a recent report, we demonstrated that L6 is able to noncovalently complex with plasmid DNA prepared at an N/P ratio of 12, and to efficiently deliver the plasmid DNA into cells.[30] Moreover, L6, also denoted as $bLFcin_6$, was shown to efficiently deliver small interfering RNA (siRNA) into cells without immunogenicity or cytotoxicity.[37] Collectively, these studies demonstrate that protein transduction mediated by nontoxic L6 CPP is a simple and efficient method for the delivery of nucleic acids and nanoparticles into cells.

QDs possess advantageous properties as probes as compared to radioactive tags or organic fluorophores (e.g., FITC, rhodamine, and cyanine dyes), and are therefore widely used in cellular imaging and labeling *in vitro* and *in vivo*.[20] Our present results with L6-mediated QD delivery into cells are consistent with recent reports.[13, 23, 26, 38] Insofar as QDs alone rarely enter cells,[23] CPPs leave a large percentage of their QD cargos in the endocytic system.[13, 26, 38]

The unique characteristics of QDs allow their use in real-time monitoring of nanoparticle bio-distribution, intracellular uptake, drug release, and long-term disposition.[39] One emerging application is the integration of QDs and drugs into a single nanoparticle formulation.[39] Alternate approaches have been taken to achieve this goal: Drug molecules can be conjugated to the QD surface, or drug molecules can be loaded in polymer nanoparticles that contain QDs.

The molecular pathways CPPs utilize for cellular entry are still subject to debate. Studies using several complementary bioassays support the notion that endocytosis and direct membrane translocation are both involved in internalization of CPPs and CPP/cargo complexes.[12, 13] In general, the cell uptake mechanism of a specific CPP is influenced by multiple factors, including the properties of the CPP (length, charge, amphiphile, residue composition, etc.), the physiochemical properties of the cargo molecule, and cell type.[40] Endocytic processes are important in most cells for nutrient absorption, cellular signaling, and gap junctional/intercellular communication.[28] If the cellular internalization is through endocytosis, CPP/cargo complexes initially accumulate inside endocytic vesicles, such as endosomes and lysosomes. If the target of the delivered cargo molecules is outside of endocytic vesicles, CPP/cargo complexes must escape into the cytosol to reach their ultimate targets. Accordingly, to effectively and efficiently deliver macromolecular cargos into cells by endocytosis, CPPs have to fulfill three critical criteria.[1] First, CPP/cargo complexes need to associate with the cell surface by electrostatic interactions. Second, the complexes must undergo internalization by endocytosis. Third, CPP/cargo complexes have to escape from the endosomal vesicles and enter the cytoplasm. The last step is the rate-limiting step of CPP protein transduction.[1] To facilitate endosomal escape after endocytosis by CPP protein transduction, various membrane-disruptive peptides and polymers, lysosomotropic agents, and fusogenic lipids have been used.[40, 41] Lysosomotropic agents generally destabilize endosomal membranes by affecting protonation (effect of low pH) or promoting fusion into the lipid bilayer of the endosomes.[40] For example, our previous data demonstrated that an endosomolytic hemagglutinin-2 (HA2) peptide derived from the influenza virus dramatically increases CPP-mediated protein entry through the release of endocytosed fusion proteins into the cytoplasm.[42] In addition, the lysosomotropic agent chloroquine was demonstrated to facilitate cellular uptake of CPP/cargo complexes and allow them to escape from endocytic vesicles into the cytoplasm.[35, 43, 44] Other chemical agents, including calcium and sucrose,[45, 46] have also been used to overcome endosome entrapment. Improving endosomal escape without increasing cytotoxicity is one of the two major challenges of CPP-mediated macromolecular delivery (target-cell specificity is the other).[1]

Some transduction enhancers, such as pyrenebutyrate[35, 47] and DMSO,[35, 48] have been employed to improve CPP transduction efficiency by increasing membrane permeability. BIT was recently introduced as a chemical enhancer that improves cellular uptake of Tat PTD and PTD-GFP fusion protein without causing membrane perforation.[19] However, the present results indicate that 0.65 mM of BIT does not affect L6-mediated QD transfection. Furthermore, we found that the cells treated with BIT showed a certain degree of membrane damage (data not shown), which is not in agreement with a previous study.[19] The reasons for this discrepancy are unclear.

5. CONCLUSION

A novel L6 (RRWQWR) CPP derived from bovine lactoferricins is able to form stable complexes with QDs at an optimized N/P ratio of 60 and to deliver QDs into human A549 cells. Classical energy-dependent endocytosis is the major route for cellular internalization of L6/QD complexes. L6 and L6/QD complexes were not cytotoxic. Thus, L6 CPP may be a safe, simple, and efficient carrier of nanoparticles or therapeutic cargos in biomedical applications.

ABBREVIATIONS

BFP	blue fluorescent protein
BIT	1,2-benzisothiazol-3(2*H*)-one
CPP	cell-penetrating peptide
CytD	cytochalasin D
DMSO	dimethyl sulfoxide
EEA1	early endosome antigen 1
EIPA	5-(*N*-ethyl-*N*-isopropyl)-amiloride
FIL	filipin III
FITC	fluorescein isothiocyanate
GFP	green fluorescent protein
LFcin	lactoferricin
MTT	3-(4,5-dimethylthiazol-2-yl)-2,5-diphenyltetrazolium bromide
NCO	nocodazole
N/P	nitrogen (NH_3^+)/phosphate (PO_4^-)
PBS	phosphate buffered saline
PTD	protein transduction domain
QD	quantum dot
RFP	red fluorescent protein
SD	standard deviation
Tat	transactivator of transcription.

Acknowledgments: This work was supported by the Center for Biomedical Science and Engineering at Missouri University of Science and Technology and the Ministry of Science and Technology, Taiwan (Grant No. MOST 104-2320-B-259-002-MY3).

References and Notes

1. P. Lonn and S. F. Dowdy, *Expert Opin. Drug Deliv*. 12, 1627 (**2015**).
2. M. Green and P. M. Loewenstein, *Cell* 55, 1179 (**1988**).
3. A. D. Frankel and C. O. Pabo, *Cell* 55, 1189 (**1988**).
4. E. Vives, P. Brodin, and B. Lebleu, *J. Biol. Chem*. 272, 16010 (**1997**).
5. F. Wang, Y. Wang, X. Zhang, W. Zhang, S. Guo, and F. Jin, *J. Control. Release* 174, 126 (**2014**).
6. P. Agrawal, S. Bhalla, S. S. Usmani, S. Singh, K. Chaudhary, G. P. Raghava, and A. Gautam, *Nucleic Acids Res*. 44, D1098 (**2016**).
7. A. Gautam, K. Chaudhary, R. Kumar, A. Sharma, P. Kapoor, and A. Tyagi, Open source drug discovery consortium, and G. P. Raghava, *J. Transl. Med*. 11, 4 (**2013**).
8. T. A. Holton, G. Pollastri, D. C. Shields, and C. Mooney, *Bioinformatics* 29, 3094 (**2013**).
9. H. Tang, Z. D. Su, H. H. Wei, W. Chen, and H. Lin, *Biochem. Biophys. Res. Commun*. 477, 150 (**2016**).
10. K. Kurrikoff, M. Gestin, and U. Langel, *Expert Opin. Drug Deliv*. 13, 373 (**2016**).
11. R. Glogau, A. Blitzer, E. Brandt, M. Kane, G. D. Monheit, and J. M. Waugh, *J. Drugs Dermatol*. 11, 38 (**2012**).
12. M. Chang, Y. W. Huang, R. S. Aronstam, and H. J. Lee, *Curr. Pharm. Biotechnol*. 15, 267 (**2014**).
13. Y. W. Huang, H. J. Lee, L. M. Tolliver, and R. S. Aronstam, *BioMed. Res. Int*. 2015, 834079 (**2015**).
14. S. D. Conner and S. L. Schmid, *Nature* 422, 37 (**2003**).
15. M. Rusnati, D. Coltrini, P. Oreste, G. Zoppetti, A. Albini, D. Noonan, F. d'Adda di Fagagna, M. Giacca, and M. Presta, *J. Biol. Chem*. 272, 11313 (**1997**).
16. I. M. Kaplan, J. S. Wadia, and S. F. Dowdy, *J. Control. Release* 102, 247 (**2005**).
17. T. A. Gottlieb, I. E. Ivanov, M. Adesnik, and D. D. Sabatini, *J. Cell Biol*. 120, 695 (**1993**).
18. J. E. Schnitzer, P. Oh, E. Pinney, and J. Allard, *J. Cell Biol*. 127, 1217 (**1994**).
19. J. L. Ma, H. Wang, Y. L. Wang, Y. H. Luo, and C. B. Liu, *Mol. Pharm*. 12, 2040 (**2015**).
20. H. Mattoussi, G. Palui, and H. B. Na, *Adv. Drug Deliv. Rev*. 64, 138 (**2012**).
21. X. Michalet, F. F. Pinaud, L. A. Bentolila, J. M. Tsay, S. Doose, J. J. Li, G. Sundaresan, A. M. Wu, S. S. Gambhir, and S. Weiss, *Science* 307, 538 (**2005**).
22. J. B. Delehanty, H. Mattoussi, and I. L. Medintz, *Anal. Bioanal. Chem*. 393, 1091 (**2009**).
23. J. K. Jaiswal and S. M. Simon, *Cold Spring Harb. Protoc*. 2015, 619 (**2015**).
24. L. Shao, Y. Gao, and F. Yan, *Sensors* 11, 11736 (**2011**).
25. B. R. Liu, Y. W. Huang, H. J. Chiang, and H. J. Lee, *J. Nanosci. Nanotech*. 10, 7897 (**2010**).
26. B. R. Liu, J. G. Winiarz, J. S. Moon, S. Y. Lo, Y. W. Huang, R. S. Aronstam, and H. J. Lee, *Colloids Surf. B Biointerfaces* 111, 162 (**2013**).
27. S. Futaki, W. Ohashi, T. Suzuki, M. Niwa, S. Tanaka, K. Ueda, H. Harashima, and Y. Sugiura, *Bioconjug. Chem*. 12, 1005 (**2001**).
28. T. Kaitsuka and K. Tomizawa, *Int. J. Mol. Sci*. 16, 26667 (**2015**).
29. T. Hitsuda, H. Michiue, M. Kitamatsu, A. Fujimura, F. Wang, T. Yamamoto, X. J. Han, H. Tazawa, A. Uneda, I. Ohmori, T. Nishiki, K. Tomizawa, and H. Matsui, *Biomaterials* 33, 4665 (**2012**).
30. B. R. Liu, Y. W. Huang, R. S. Aronstam, and H. J. Lee, *PLoS One* 11, e0150439 (**2016**).
31. W. S. Sanders, C. Ian Johnston, S. M. Bridges, S. C. Burgess, and K. O. Willeford, *PLoS Comput. Biol*. 7, e1002101 (**2011**).
32. C. P. Chen, J. C. Chou, B. R. Liu, M. Chang, and H. J. Lee, *FEBS Lett*. 581, 1891 (**2007**).
33. B. R. Liu, J. F. Li, S. W. Lu, H. J. Lee, Y. W. Huang, K. B. Shannon, and R. S. Aronstam, *J. Nanosci. Nanotechnol*. 10, 6534 (**2010**).
34. B. R. Liu, Y. W. Huang, J. G. Winiarz, H. J. Chiang, and H. J. Lee, *Biomaterials* 32, 3520 (**2011**).
35. B. R. Liu, S. Y. Lo, C. C. Liu, C. L. Chyan, Y. W. Huang, R. S. Aronstam, and H. J. Lee, *PLoS One* 8, e67100 (**2013**).
36. W. S. Rasband, ImageJ. U.S. National Institutes of Health, Bethesda, Maryland, USA (**1997–2016**), https://imagej.nih.gov/ij/.
37. B. Fang, H. Y. Guo, M. Zhang, L. Jiang, and F. Z. Ren, *FEBS J*. 280, 1007 (**2012**).
38. B. R. Liu, H. H. Chen, M. H. Chan, Y. W. Huang, R. S. Aronstam, and H. J. Lee, *J. Nanosci. Nanotechnol*. 15, 2067 (**2015**).
39. S. Chen, X. Hao, X. Liang, Q. Zhang, C. Zhang, G. Zhou, S. Shen, G. Jia, and J. Zhang, *J. Biomed. Nanotechnol*. 12, 1 (**2016**).
40. C. P. Cerrato, K. Kunnapuu, and U. Langel, *Expert Opin. Drug Deliv*. 14, 245 (**2017**).

41. A. Komin, L. M. Russell, K. A. Hristova, and P. C. Searson, *Adv. Drug Deliv. Rev*. 110–111, 52 **(2017)**.
42. J. S. Liou, B. R. Liu, A. L. Martin, Y. W. Huang, H. J. Chiang, and H. J. Lee, *Peptides* 37, 273 **(2012)**.
43. S. Yang, D. J. Coles, A. Esposito, D. J. Mitchell, I. Toth, and R. F. Minchin, *J. Control. Release* 135, 159 **(2009)**.
44. B. R. Liu, J. S. Liou, Y. W. Huang, R. S. Aronstam, and H. J. Lee, *PLoS One* 8, e64205 **(2013)**.
45. T. Shiraishi, S. Pankratova, and P. E. Nielsen, *Chem. Biol*. 12, 923 **(2005)**.
46. S. Abes, D. Williams, P. Prevot, A. Thierry, M. J. Gait, and B. Lebleu, *J. Control. Release* 110, 595 **(2006)**.
47. T. Takeuchi, M. Kosuge, A. Tadokoro, Y. Sugiura, M. Nishi, M. Kawata, N. Sakai, S. Matile, and S. Futaki, *ACS Chem. Biol*. 1, 299 **(2006)**.
48. A. A. Gurtovenko and J. Anway, *J. Phys. Chem. B* 111, 10453 **(2007)**.

Received: 13 August 2017. Accepted: 29 January 2018.